Estimating the Spectra of Small Events for the Purpose of Evaluating Microseismic Detection Threshholds

N. Ackerley, Nanometrics, Inc., Kanata, Canada
NickAckerley@nanometrics.ca

GeoConvention 2012:Vision

Summary

A crucial question which comes up over and over in the design of microseismic survey networks is: “What is the smallest magnitude event which we will be able to detect?” In order to answer this question, of course, to have reliable estimates of the spectrum of typical ground motion at a given site. Less obvious are the difficulties in modeling event spectra. This poster addresses this issue in two steps. First, the theoretical spectra of Brune (1970) are reconciled with the measured spectra of Clinton and Heaton (2002). Second, the operations required to scale these spectra for comparison with power spectral densities of ground motion and sensor self-noise are shown.

It turns out that the intrinsic attenuation between the source and receiver, expressed in terms of a quality factor, is by far the most important factor in determining the high-frequency roll-off of a seismic spectrum, much more important than the Brune corner frequency.

It is important to appreciate the fact that real event spectra have significant scatter, the scaling problem inherent in comparing different measures of earthquake magnitude and the role of trigger algorithms.

Given this working model and an understanding of how to use it, it becomes possible to make estimates of the minimum magnitude at which 50% of the events are likely to be detected at a given epicentral distance. Conversely, given such a model and a required minimum event size which must be detected with 50% probability, one can state the required station spacing.

In particular it is shown that a broadband seismometer in the class of the Nanometrics Trillium Compact has an intrinsic detection limit of about M-2 at 2 km hypocentral distance. In contrast, a typical low-gain geophone has an intrinsic detection limit of about M-1 at the same hypocentral distance.

Introduction

The question of detection limits bears heavily on the design of microseismic monitoring arrays. These arrays are essential for ensuring the safety and efficiency of emerging technologies which involve injecting materials underground at high pressure, such as hydraulic fracturing, geothermal power generation and carbon sequestration. The number of instruments required and their optimal separation depends on the observed site noise, the sensor self-noise, and the minimum event size which must be detected.

As it is colloquially known, the Richter magnitude is a relatively widespread way of understanding the size of events. It is therefore is useful for communicating seismic and other risks related to various new technologies such as hydraulic fracturing, geothermal power and carbon sequestration.

The number of events which a microseismic monitoring network can detect in a given time frame is crucial, because it will determine the quality of picture which can be generated of the stimulated volume and because more events will provide a better basis for a frequency of recurrence versus magnitude scaling law. This means the smaller events which can be detected the better. So the question is, then: what is the smallest event a given network can detect? Fundamentally, therefore, there is a need for reliable estimates of ground motion as a function of frequency, magnitude and epicentral distance.

Theory

Many authors, recently for example Goertz (2011) and Eaton (2011), refer to the model for the spectra of seismic events developed by Brune (1970). It is not a trivial matter to reconcile these spectra with actual ground motion, however. Reasonable estimates must be made of the various parameters in the amplitude spectrum and then a means is needed for estimating the spectrum for real events.

Amplitude Spectra

The model developed by Brune (1970) gives the displacement spectrum as:

$$\Omega(f) = \frac{\Omega_0}{\sqrt{1 + \left(\frac{f}{f_c}\right)^2}}$$

This is the Fourier transform with respect to time of the displacement of some point in the far field vs. time. Because computing the Fourier transform involves multiplying the displacement by an increment of time as the function is integrated over time, the units are m·s, not m, as one might expect for a function called a displacement spectrum.

The low-frequency plateau Ω_0 is proportional to the seismic moment M_0. For an inhomogeneous medium the relationship between the two is given by Aki and Richards (2002):

$$\Omega_0 = \frac{F_R S_a}{4\pi\sqrt{\rho_r * \rho_s * V_r * V_s^5}} \frac{M_0}{r_h}$$

The various parameters in this equation are:

- The phase velocities of the media near the source and receiver, denoted by V_r and V_s. The phase in question can be either the P-wave or the S-wave, but we will concentrate primarily on the S-waves. For a receiver at the surface the velocity will typically be significantly lower than that at the source, which is why we're using the approximation for inhomogeneous media.
- The densities of the media near the source and receiver, denoted by ρ_s and ρ_r. The density can be approximated for a broad range of lithology given the S-wave velocity using the rule proposed by Gardner (1974),

  $$\rho = 0.23\beta^{0.25},$$

  where the S-wave velocity β is expressed in feet/second and the resulting density is expressed in g/cm^3. This is the approach used in this article.
- The factor $1 \leq F_R \leq 2$ accounts for the effect of the proximity of the receiver to the surface. It should be set to $F_R = 2$ for sensors installed at the surface.
- The factor S_a accounts for the radiation pattern from the fault. Although the radiation patterns are different for P- and S- waves, in both cases the amplitude as a function of azimuth is a rectified sine wave, so we will use the average of the radiation pattern and set $S_a = 2/\pi$.
- The hypocentral distance r_h accounts for the effects of geometrical spreading in three dimensions. It must take into account both the epicentral distance and the depth for nearby events.
- The seismic moment M_0 relates directly to the physical dimensions of the fault and to the measured magnitude in the far field, as described in what follows.

The seismic moment is defined as the product of the fault area, A, the average total slippage, $\bar{u}$, and the shear modulus of the rocks involved, μ.

$$M_0 = \mu\bar{u}A$$

Since seismic moment is a measure of the energy released by an earthquake, the units are joules. Of course we don't know the dimensions or other characteristics of the event *a priori* but we do know its relationship to the moment magnitude.

Earthquake magnitudes can be estimated using a variety of methods. Many of these methods, such as the original local magnitude M_L of Richter and Gutenberg and the teleseismic surface-wave magnitude M_S saturate at large magnitudes. That is, past a certain magnitude, for these measures of magnitude, even though the energy released increases, the measured magnitude does not. At the same time, all of these magnitude estimates are really trying to estimate the energy released by the earthquake. They can therefore be used somewhat interchangeably, because all of the magnitude estimates are scaled to be equivalent to M_L in the range where it is not saturating. See Choy and Boatwright (2009).

The energy released by an earthquake of moment magnitude M_W is

$$M_0 = 10^{\frac{3}{2}M_W + 9}$$

The corner frequency for a circular fault, according to Brune (1970) can be estimated using:

$$f_c = \frac{K_p}{2\pi}\frac{V_s}{R_0}$$

Where the radius of the fault R_0 can be estimated from the magnitude of the seismic moment, M_0, and the stress drop σ_0, according to Abercrombie (1995):

$$R_0 = \sqrt[3]{\frac{7}{16}\frac{M_0}{\sigma_0}}$$

According to Brune (1970) and others, stress drop is a remarkably constant quantity, at least for the larger events they were studying.

At high frequencies the spectrum decays as $1/f^2$. Aki and Richards (2002) argue that this can be understood as being a product of the effect of the finite length over which the fault propagates and the finite rise time of the slip. However the classic Brune spectrum was generalized by Abercrombie (1995) in an attempt to explore the possibility of the high-frequency roll-off having different slopes, n, and the corner frequency having different degrees of sharpness, γ, and to include the effect of attenuation via a quality factor, Q:

$$\Omega(f) = \frac{\Omega_0}{\left(1 + \left(\frac{f}{f_c}\right)^{\gamma n}\right)^{\frac{1}{\gamma}}} e^{-\frac{\pi f r_h}{Q\sqrt{V_s V_r}}}$$

The quality factor turns out to be critically important in determining the roll-off of the spectra at high frequencies.

It is important to note that this model is particular to the strike-slip mechanism which is dominant in tectonic earthquakes. Implosions and explosions, for example, are characterised not by shear rupture but by sudden compression or tension, produce only P-waves, and have higher corner frequencies. Volcanic earthquakes have their own set of source mechanisms in which magma flows play a role. Different estimates of magnitude require different scaling factors for different source mechanisms. The bottom line is that there may be source mechanisms unique to geothermal power generation or hydraulic fracturing, producing source spectra distinct from those of tectonic earthquakes.

Octave Band-Passed Peak Spectra

In the course of investigating the relative utility of accelerometers and velocity meters for the measurement of strong motion due to earthquakes, Clinton and Heaton (2002) assembled an earthquake database and used octave-wide band-pass filters to determine the peak amplitudes as a function of frequency for a variety of magnitudes and epicentral distances. This method avoids the problem of having to pick a duration over which to compute a power spectrum.

Figure 1 graphically illustrates the methodology of Clinton and Heaton, for the case of events of magnitude M3.5 at an epicentral distance of 100 km. Similar curves were developed and published for M1.5 to M7+ and epicentral distances of 10 km, 100 km and 3000 km.

Although the spectra of Clinton and Heaton were developed for comparison to clip levels, they are just as useful for comparison to noise floors, because the problem of triggering events boils down to detecting a peak amplitude, typically computed as a short-term average, with respect to the RMS or long-term average of the background noise.

Noting the scatter in Figure 1, the event spectrum clearly approximates the median amplitudes for a given size of event as a function of frequency. Half of the time, an event of the given magnitude will produce larger amplitudes, and half the time the amplitudes will be smaller.

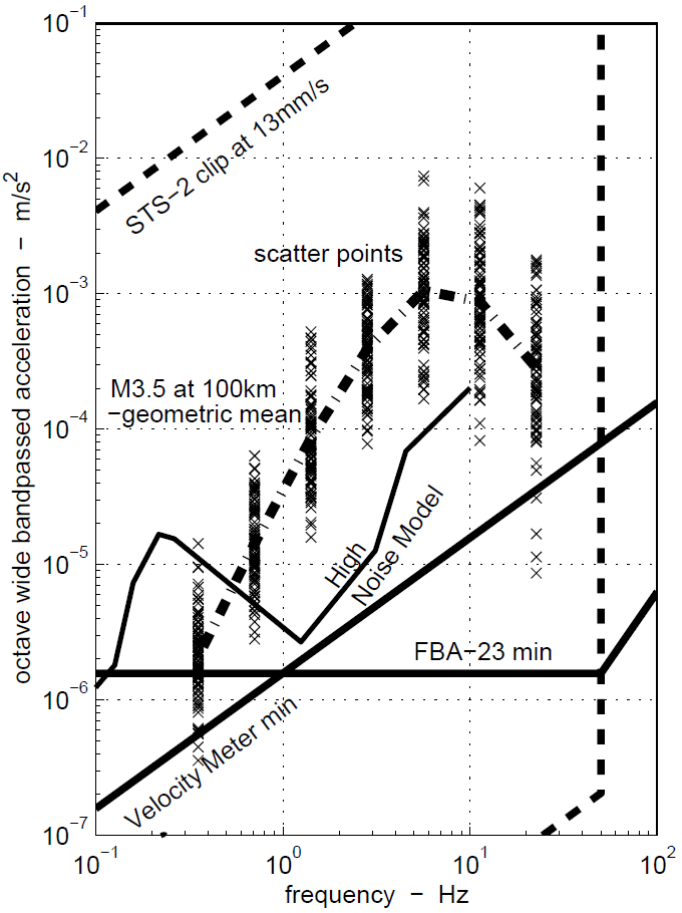

Figure 1: Method of Obtaining Median Power Spectra
This figure is reprinted from Clinton and Heaton (2002), Figure 4. The caption in the original reads, in part: "Data scatter and geometric mean for M3.5 at 100 km. The crosses are the data points, and their geometric mean is represented by the thick dash-dotted line."

Aki and Richards (2002) show that the maximum amplitude of a wavelet can be approximated by:

$$x_{max}(\omega) = 2|X(\omega)|(f_u - f_l)$$

Where ω is the angular frequency at the center of the band-pass filter bounded by the frequencies f_l and f_u.

We will choose relative bandwidth as a fraction of the center frequency of the band, so that

$$x_{max}(f) = 2|X(f)|k_{RBW}f$$

In the case of displacement spectra, this transformation takes the units from m·s back to m.

Finally, for comparison units of acceleration or velocity, we use the simple relationships relating amplitudes of sine waves:

$$V(\omega) = \omega D(\omega)$$
$$A(\omega) = \omega V(\omega)$$

These relations apply equally well to amplitude spectra or power spectra.

At low frequencies, the equivalent acceleration amplitude spectrum of an event should therefore have a slope of 40 dB/ decade.

Comparison to Power Spectra

The noise floors of well-constructed seismometers are stationary. That is to say that the noise floor doesn't change with time so that although the noise is random, the power spectral density is constant over time.

In order to compare an amplitude spectrum to a power spectrum, we use a relative bandwidth factor k_{RBW} time the frequency f to compute the RMS signal in a given band, and a crest factor k_{crest} to convert the resulting RMS signal into a peak amplitude.

$$x_{max}(f) = k_{crest}\sqrt{P(f)k_{RBW}f}$$

And since a displacement power spectrum will have units of m^2/Hz, the resulting amplitude is in m. Since Clinton and Heaton chose octave band-pass filters, we will set the relative bandwidth factor to:

$$k_{RBW} = \sqrt{2} - \frac{1}{\sqrt{2}} = \frac{1}{\sqrt{2}}$$

According to Bormann (2009b) the probability distribution of a typical earthquake signal is Gaussian and the peak amplitude of a band-passed Gaussian signal is related to the RMS value by:

$$k_{crest} = \sqrt{\frac{\pi}{2}}$$

At low frequencies, the equivalent acceleration PSD to the amplitude spectrum of an event should have a slope of 50 dB/ decade.

Comparison of Modeled and Measured Spectra

We will follow Goertz (2011), since our ultimate interest is in deep sedimentary strata and set

- V_s = 3400 m/s
- V_r = 3060 m/s

Goertz (2011) uses a quality factor of 150. While it is beyond the scope of this paper to do an extensive survey, this seems like a rather high value for events at close proximity to a surface receiver. For example Eaton (2011) reports quality factors between 22.5 and 25. For the comparison with Clinton and Heaton the best fit with the measured spectra was obtained when the quality factor was varied linearly from 75 to 100 for the M6.5 to M1.5 event spectra.

Similarly Goertz chooses a stress drop of 10 MPa, which is significantly higher than the value of 1 MPa which Brune found representative. Good agreement between model and measurement was obtained for a stress drop of 3 MPa.

The seismic moment released by a M1.5 event is 1.8×10^{11} J, the source radius is approximately 30 m and the Brune corner frequency is 40 Hz. The resulting spectra are compared with the spectra published by Clinton and Heaton (2002) for 10 km epicentral distance in Figure 2.

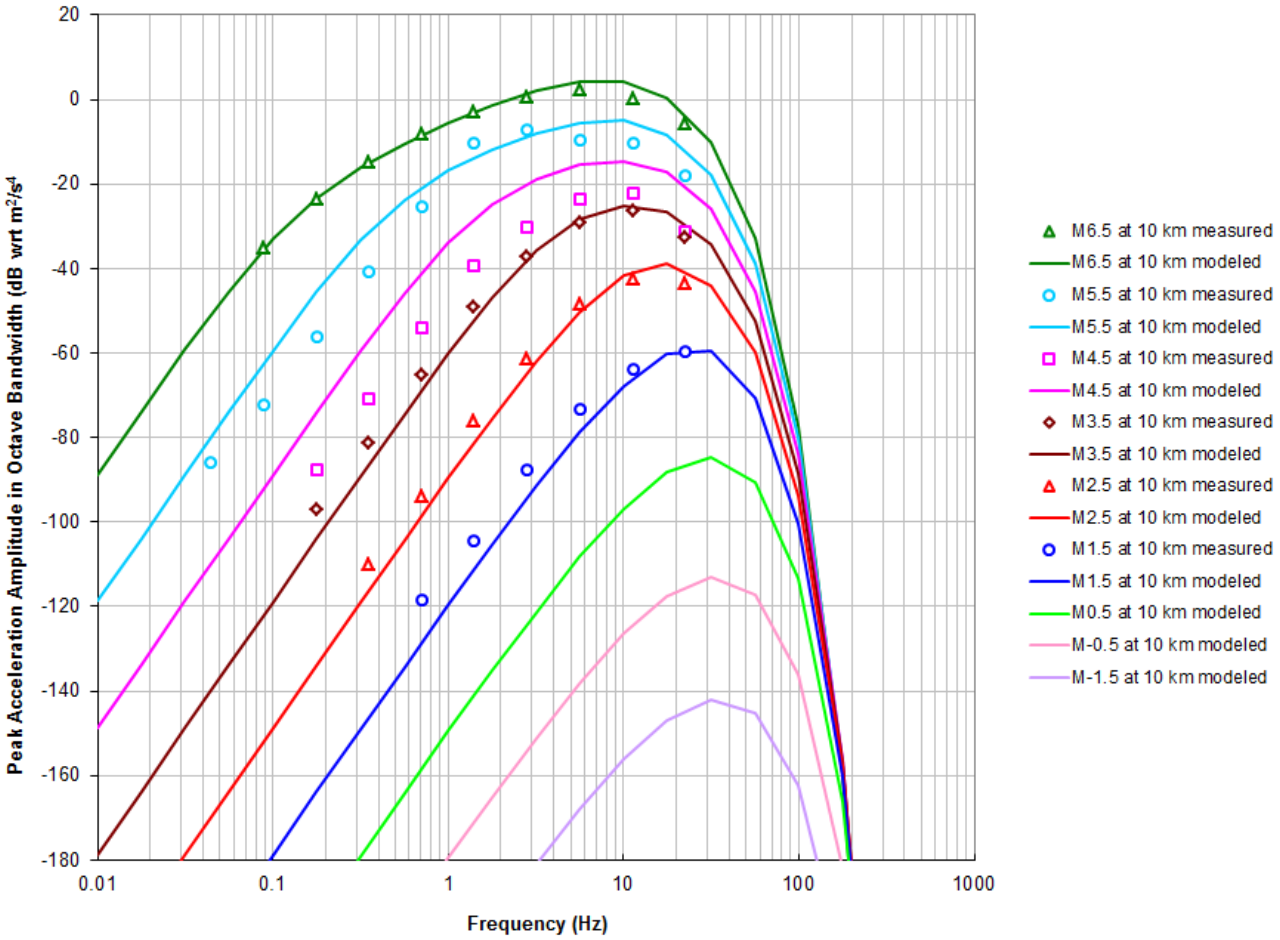

Figure 2: Comparison of Model to Measurements for 10 km Epicentral Distance
Models assume $\boldsymbol{V_s}$ = 3400 m/s, $\boldsymbol{V_r}$ = 3060 m/s, $\boldsymbol{\sigma_0}$ = 3 MPa and Q between 75 and 100.

With the fine-tuning mentioned, correspondence between measured and modeled spectra is excellent. The most glaring anomaly is that the measured low-frequency asymptotes for M4.5 and M5.5 tend to be lower than the model predicts while those for M1.5, M2.5 and M3.5 events tend to be higher. Ground motion amplitudes at low frequencies should surely scale strictly with magnitude. It is possible that the events selected for the database by Clinton and Heaton have some built-in bias relating to their size. Perhaps one set of events was obtained primarily from one instrumentation network and/or originating in one set of types of faults while the other set of events was obtained from another.

Having noted this anomaly, the slope of the low-frequency asymptote is correct, and although data on the shape of the roll-off at high frequency does not extend to frequencies high enough to be sure, there is reasonable agreement with the available data.

A success of the model is the predicted flattening of the spectra in the mid-band at the largest magnitude. At these magnitudes the Brune spectra corner frequencies are quite low so they are easily separated from the roll-off at high frequencies due to attenuation.

Conversely, for the smallest events, the Brune corner is at a higher frequency then the corner due to attenuation, so the latter is much more important in determining what frequencies contain the most seismic energy. This is significant because it means that in estimating the spectra of small events it is the attenuation which matters, not the stress drop.

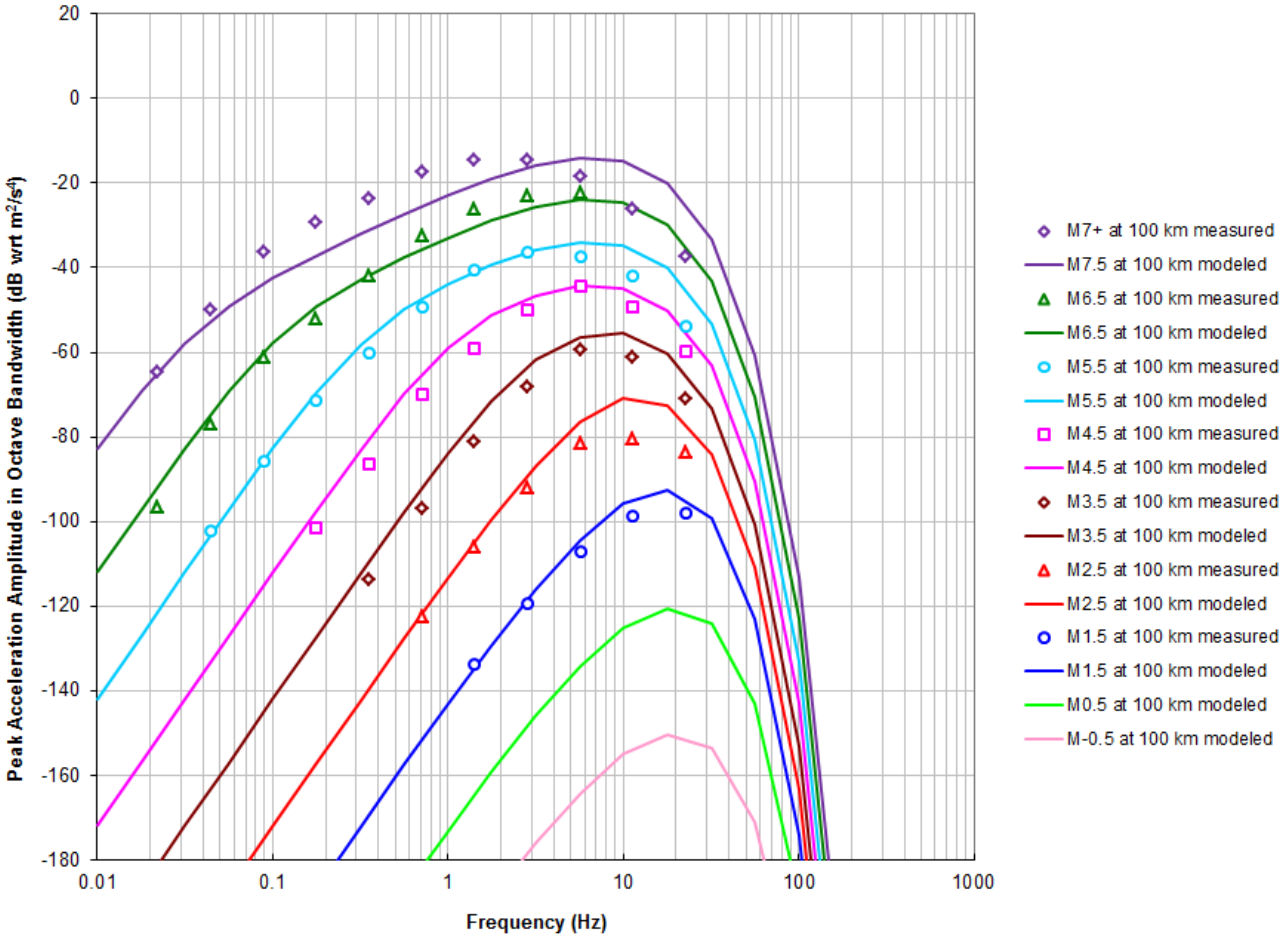

Figure 3: Comparison of Model to Measurements for 100 km Epicentral Distance
Models assume V_s = 3900 m/s, V_r = 3060 m/s, σ_0 = 1 MPa and Q = 600.

For epicentral distances on the order of 100 km, the model is compared to Clinton and Heaton's measurements in Figure 3. The shear wave velocity at the receiver was chosen to be 3900 m/s, and the quality factor was set to 600, following the PREM 1D model of the earth for 15-24 km depth, as per Bormann (2009c). These parameters fit the data much better than those used for 10 km epicentral distances, and make sense since the events are likely to have deeper foci.

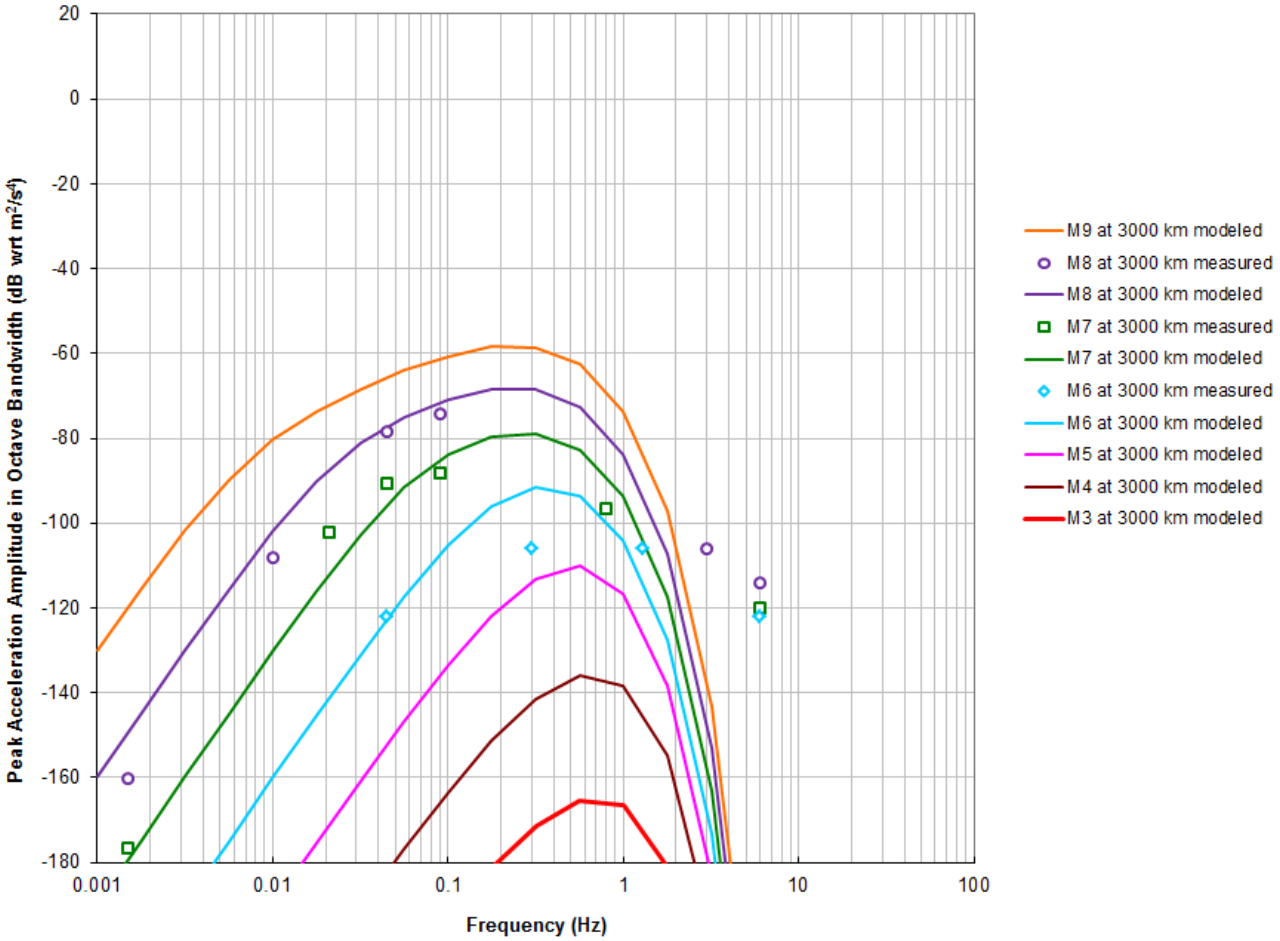

Figure 4: Comparison of Model to Measurements for 3000 km Epicentral Distance
Models assume V_s = 4500 m/s, V_r = 3060 m/s, σ_0 = 1 MPa and Q = 600.

For epicentral distances on the order of 3000 km, the model is compared to Clinton and Heaton's measurements in Figure 4. The shear wave velocity at the receiver was chosen to be 4500 m/s, and the quality factor was set to 600, approximating the PREM 1D model of the earth for 24-80 km depth, as per Bormann (2009c). Note the shift to lower frequencies in comparison with the previous two figures.

The fit is reasonable for very long periods, but is poor above 1 Hz. The number of events available to Clinton and Heaton was admittedly very small for the se teleseismic events, so that may be a factor. Another possibility is that surface waves have become dominant at these huge epicentral distances and frequencies, because they don't decay as rapidly with distance as body waves.

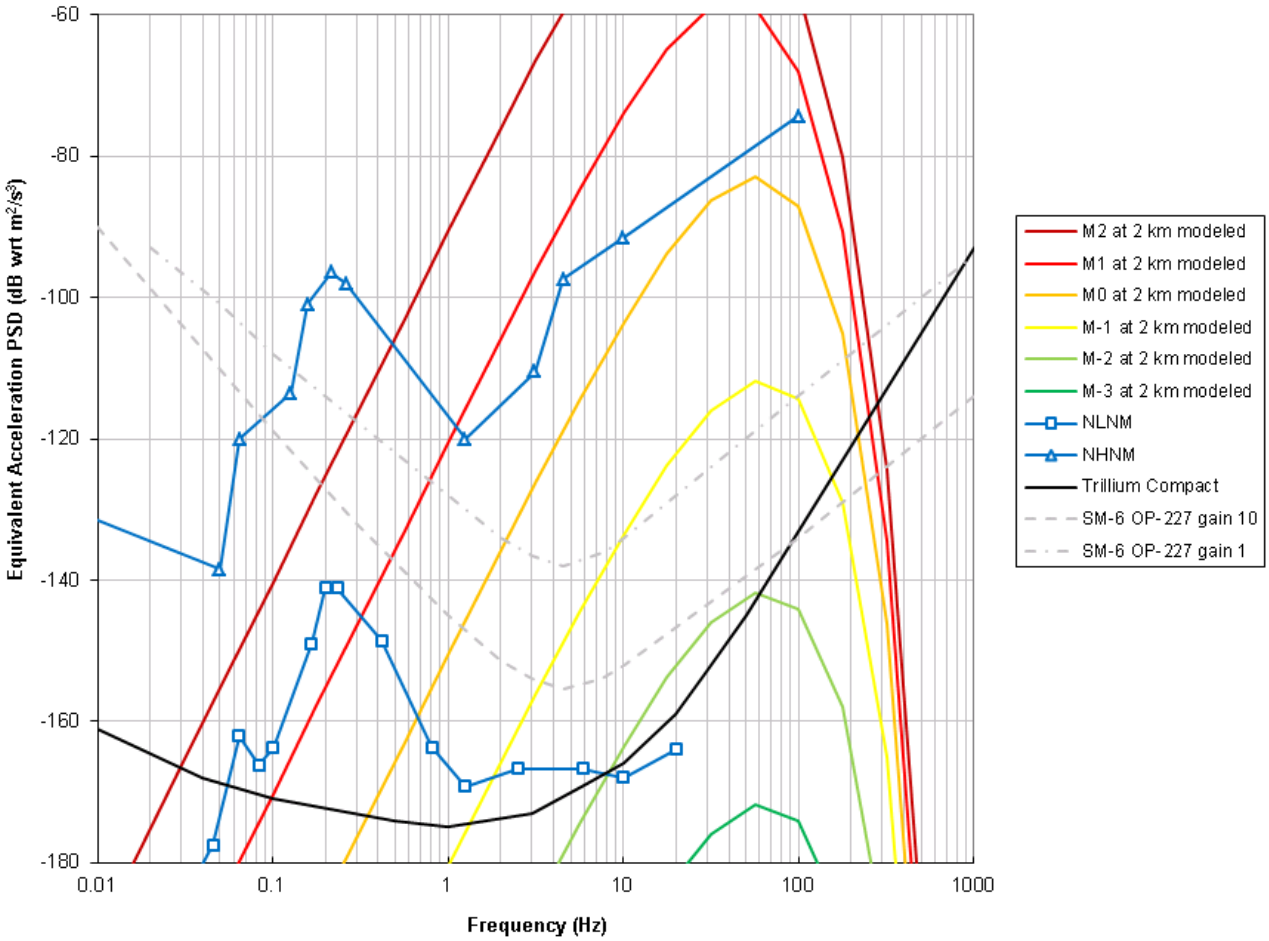

Figure 5: Detection Thresholds for Small Events
Models assume V_s = 3400 m/s, V_r = 3060 m/s, σ_0 = 3 MPa and Q = 50.

Figure 5 shows the extrapolation of this same model of small events to smaller magnitudes and closer epicentral distances. Note the difference in the vertical axis units, resulting in a different slope for the low-frequency asymptotes. A hypocentral distance of 2 km was chosen as representative for a gas-bearing shale hydraulic fracturing operation. The quality factor was fixed at 50 for all events shown, but would in practice need to be more exactly characterised for a given microseismic monitoring network deployment. The stress drop was set at 1 MPa, but it hardly matters for such small events.

Notwithstanding excess ground motion due to site noise, we can conclude that a Trillium Compact should be able to detect an M-2 event more than 50% of the time, but not an M-3 event at this range. A high-gain geophone will similarly be able to detect an M-2 event significantly less than 50% of the time, and a low-gain geophone will be able to detect M-1 events, but not M-2 events.

Included in Figure 5 are the NLNM and NHNM, models of earth noise at typical good sites. In practice, a seismometer, properly installed just about anywhere on Earth, will record site noise spectra between these two lines. The site has to be quite good, typically on bedrock and/or underground, to approach the NLNM. Although further improvement is possible through stacking in practice the detection limits outlined in the previous paragraph are going to tend to be optimistic.

Pre-injection site surveys are clearly going to be indispensable. First, it is critical to determine levels of site noise and re-site instruments as needed to obtain the lowest possible site noise. Second, such a survey allows the surveyor to ascertain the appropriate phase velocities and quality factors to use for modeling of small events. With such data in hand it becomes possible to determine the detection threshold of a given network and the minimum required station spacing to detect events of a given size.

Conclusions

This poster develops and documents a detailed model like that of Brune (1970) and validates it by comparison with the work Clinton and Heaton (2002). The same model is then used to generate event spectra for smaller, closer events, appropriate for assessing the detection limit of a hypothetical seismograph network with low site noise. A network composed of Trillium Compacts for example, is capable of detecting M-2 events at 2 km hypocentral distance, for example.

To assess the detection limit of a real network or to carefully set the optimum number and spacing of seismometers, a preliminary survey is indispensable. Such a survey allows the site noise to be assessed and sensors relocated on the surface or below ground as needed to achieve stated design goals. It furthermore permits measurement of the quality factor which is so crucial to the high-frequency roll-off of the event spectra, as well as the relevant phase velocities.

References

Gutenberg, B., and C. F. Richter (1956) *Magnitude and energy of earthquakes*, Ann. Geofis., Vol. 9, pp. 1-15.

Brune, J. (1970) *Tectonic Stress and the Spectra of Seismic Shear Waves from Earthquakes*, J. Geophys. Res., Vol. 75, No. 26, pp. 4997-5009.

Gardner, G. H. F., L. W. Gardner, and A. R. Gregory (1974) *Formation velocity and density - The diagnostic basics for stratigraphic traps*: Geophysics, Vol. 39, pp. 770–780

Kanamori, H. (1983). *Magnitude scale and quantification of earthquakes*. Tectonophysics, 93, 185-199.

Peterson, J. (1993) *Observations and modelling of background seismic noise*. Open-file report 93-322, U. S. Geological Survey, Albuquerque, New Mexico.

Abercrombie, R., (1995), *Earthquake source scaling relationships from -1 to 5 ML, using seismograms recorded at 2.5 km depth*, J. Geophys. Res., Vol. 100, pp. 24015-24036.

Clinton, F. and T. Heaton (2002) *Potential Advantages of a Strong Motion Velocity Meter Over a Strong Motion Accelerometer*. Seismological Research Letters, Vol. 73 No. 3, pp. 332-342.

Aki, K. and P. Richards (2002), *Quantitative Seismology*, 2nd Ed., University Science Books.

McNamara, D. and R. Buland (2004) *Ambient Noise Levels in the Continental United States*, Bull. Seism. Soc. Am., Vol. 94, No. 4, pp. 1517-1527.

Strollo, A., S. Parolai, K.-H. Jäckel, S. Marzorati, and D. Bindi (2008) *Suitability of Short-Period Sensors for Retrieving Reliable H/V Peaks for Frequencies Less Than 1 Hz*, Bull. Seism. Soc. Am., Vol. 98, No. 2, pp. 671-681.

Bormann, P. (2009a) *Magnitude of seismic events*, In: Bormann, P. (Ed.). New Manual of Seismological Observatory Practice (NMSOP-1), IASPEI, GFZ German Research Centre for Geosciences, Potsdam, Section 3.2, pp. 16-49.

Choy, G. and J. Boatwright (2009) *Radiated seismic energy and energy magnitude*, In: Bormann, P. (Ed.). New Manual of Seismological Observatory Practice (NMSOP-1), IASPEI, GFZ German Research Centre for Geosciences, Potsdam, Section 3.3, pp. 50-57.

Bormann, P. (2009b) *Seismic Signals and Noise*, In: Bormann, P. (Ed.). New Manual of Seismological Observatory Practice (NMSOP-1), IASPEI, GFZ German Research Centre for Geosciences, Potsdam, Chapter 4.

Bormann, P. (2009c) *Global 1-D Earth Models*, In: Bormann, P. (Ed.). New Manual of Seismological Observatory Practice (NMSOP-1), IASPEI, GFZ German Research Centre for Geosciences, Potsdam, Datasheet 2.1.

Goertz, A., K. Cieślik, E. Hauser, G. Watts, S. McCrossin and P. Zbasnik (2011) *A combined borehole/surface broadband passive seismic survey over a gas storage field*, SEG San Antonio 2011 Annual Meeting, pp. 1488-1492.

Eaton (2011) *Q determination, corner frequency and spectral characteristics of microseismicity induced by hydraulic fracturing*, SEG San Antonio 2011 Annual Meeting, pp. 1555-1559.